수의학석사 학위논문

Single-slab 3D double inversion recovery for magnetic resonance brain imaging in clinically healthy dogs

임상적으로 건강한 개에서 단일 슬랩 삼차원 이중역전회복을 이용한 뇌 자기공명영상 평가

2023년 02월

서울대학교 대학원

수의학과 임상수의학 전공

제 미 성

Single-slab 3D double inversion recovery for magnetic resonance brain imaging in clinically healthy dogs

지도교수 윤 정 희

이 논문을 수의학석사 학위논문으로 제출함

2022년 12월

서울대학교 대학원

수의학과 임상수의학 전공

제 미 성

제미성의 수의학석사 학위논문을 인준함

2023년 01월

위 원 장 _____ (인)

부위원장 _____ (인)

위 원 _____ (인)

Abstract

Single-slab 3D double inversion recovery for magnetic resonance brain imaging in clinically healthy dogs

Miseong Je
Major in Veterinary Clinical Sciences
Department of Veterinary Medicine
The Graduate School
Seoul National University

In veterinary medicine, magnetic resonance imaging (MRI) is widely used for brain imaging. But complicate structures of brain tissues may cause some artifacts such as partial volume averaging in conventional sequences. As a resolution to this problem, several studies about double inversion recovery (DIR) sequences have been reported in human medicine. However, published clinical studies about brain MRI using DIR sequences in dogs are currently lacking. The purpose of this study was to evaluate the magnetic resonance features of single-slab 3D DIR sequence in the normal canine brain. Five Beagle dogs were sampled and the following pulse

sequences were acquired for each: (1) Spin echo T2-weighted (T2W), (2) fluid attenuated inversion recovery (FLAIR), (3) gray matter (GM) selective, and (4) white matter (WM) selective single-slab 3D DIR sequence. For qualitative analysis, the distinction between gray and white matter, presence and severity of the image artifacts were assessed for each pulse sequence. In addition, reconstructed images of single-slab 3D DIR sequences were assessed qualitatively. For quantitative analysis, contrast ratios (CRs), signal-to-noise ratios (SNRs), and contrast-to-noise ratios (CNRs) of the GM, WM and CSF were measured for each pulse sequence.

GM selective 3D DIR was superior to T2W and FLAIR in delineating the boundaries between GM and WM in the overall brain area. Whereas WM selective 3D DIR depicted better gray-white matter distinction than T2W and FLAIR at the level of the medulla oblongata, where T2W and FLAIR images showed severe partial volume averaging artifacts. The 3D DIR images generally showed less artifacts than other sequences, and the reconstructed sagittal and dorsal images of these sequences had same spatial resolution as the original transverse images, without any image degradation. Both gray and white matter selective 3D DIR sequences suppressed unwanted signals well and consequently provided high contrast between gray and white matter. Findings from this study could serve as background for further studies about DIR sequences for evaluating brain diseases in dogs.

Keywords: Brain; Dog; Double inversion recovery; Magnetic resonance imaging

Student Number: 2021-23751

Table of Contents

Introduction

In veterinary medicine, various magnetic resonance imaging (MRI) sequences are used for evaluation of the brain diseases (Robertson, 2011). Because of the high soft tissue resolution and utility of specialized sequences, MRI is the preferred modality for brain imaging (Kraft et al., 1989; Hecht et al., 2010). However, it should be considered that complicatedly folded brain structure may cause some imaging artifacts. One of the most common artifacts encountered in clinical situation is partial volume averaging artifact, which easily occurs at the curved interface of different brain structures, and it can be manifested as pseudolesions (Mai, 2018). Conversely, true lesions might be obscured due to the partial volume averaging, especially in lesions adjacent to cerebrospinal fluid (CSF) (Turetschek et al., 1998). For these reasons, errors during interpretation of the MR images could happen with conventional MRI sequences such as T2-weighted (T2W) and fluid attenuated inversion recovery (FLAIR) (Geurts et al., 2005; Almutairi et al., 2020). As a supplement to these sequences, double inversion recovery (DIR) sequence has been introduced in several human studies (Geurts et al., 2005; Hamed et al., 2019; Almutairi et al., 2020). In the DIR sequence, two different 180° inversion radiofrequency (RF) pulses are applied before a classic fast or turbo spin echo acquisition, allowing two tissues to be nulled simultaneously (Redpath et al., 1994). Thus, DIR can selectively depict gray or white matter and was known for providing markedly high contrast resolution between gray and white matter with superior delineation in human patients (Redpath et al., 1994; Turetschek et al., 1998).

Especially, GM selective DIR, which selectively images GM by suppressing the signals from both WM and CSF, has been reported to provide better conspicuity of cortical and subcortical lesions in various central nervous system (CNS) diseases than other MR techniques (Umino et al., 2019).

DIR imaging was initially introduced using two-dimensional (2D) multislice sequences at 1.5-Tesla (T) (Redpath et al., 1994; Bedell et al., 1998; Turetschek et al., 1998). However, because of the complex morphology of the brain, three-dimensional (3D) MR imaging with high spatial resolution is preferable to 2D MR imaging. Some studies have reported that a multislab 3D DIR sequence improves the spatial resolution and detection of intracortical lesions, but presence of flow artifacts and signal intensity differences between slabs cannot be resolved with multislab 3D sequence (Boulby et al., 2004; Geurts et al., 2005; Pouwels et al., 2006). Single-slab 3D DIR sequence, on the other hand, has a long echo train and variable flip angles for refocusing RF pulses, which covers whole brain with high quality and without flow artifacts from CSF or blood (Pouwels et al., 2006). Consequently, multislab 3D DIR sequence was replaced by single-slab 3D DIR sequence (Umino et al., 2019).

In human medicine, DIR sequences have been widely used for evaluating many neurologic diseases including multiple sclerosis, epilepsy, and Alzheimer's disease, all of which show cortical lesions or changes in cortical thickness or volume (Jahng et al., 2016; Umino et al., 2019; Sun et al., 2021). However, to the authors' knowledge, published clinical studies about brain MRI using DIR sequences in dogs are currently lacking. The purpose of this study was to evaluate

the magnetic resonance features of single-slab 3D DIR sequences in the normal canine brain. Authors hypothesized that single-slab 3D DIR sequences, either gray or white matter selective, would provide higher tissue contrast resolution than conventional T2W and FLAIR sequences, and would identify the exact boundary between brain tissues with less artifacts in clinically healthy dogs.

Materials and Methods

1. Study design and description of dogs

This investigation was a prospective, methods comparison, exploratory study. Five purpose-bred healthy, intact male Beagle dogs were used in the study. The median age was 4 years (range, 4 - 5 years) and the median weight was 14 kg (range, 12.8 – 15.5 kg). For each dog, the screening tests including physical and neurological examination, thoracic radiography and abdominal ultrasonography were done prior to the procedures by a veterinarian (M.S.J.) with 2 years of radiology experience. All the procedures performed in the study were approved by the Seoul National University Institutional Animal Care and Use Committees (SNU-220807-1).

2. Data recording: Brain MRI protocol

Magnetic resonance imaging examinations were performed with the dogs under general anesthesia, using a 1.5-T MR scanner (GE Signa, 1.5T, GE healthcare). Anesthetic protocols were the following: medetomidine (0.01 mg/kg IM, Domitor, Zoetis) was used for premedication, alfaxalone (2.0 mg/kg IV, Alfaxan, Jurox Pty Ltd) for induction, and isoflurane (Ifran, Hana Pharm) for maintenance. Noninvasive blood pressure, oxygen saturation, heart rate, body temperature, and end-tidal carbon dioxide concentration were monitored during the anesthesia.

The dogs were positioned in sternal recumbency on a 8-channel phased-array knee coil. Spin echo T2W, FLAIR, GM and WM selective single-slab 3D DIR images were obtained in transverse plane from each dog. Table 1 details the parameters that were used for each sequence. To reduce the acquisition time for 3D DIR sequences, number of excitations (NEX) was adjusted from 4 to 2. The acquisition time for each sequence was automatically recorded. After the examination, complications related to the anesthesia were monitored for 5 days in each dog.

Table 1. Pulse sequence parameters used for brain magnetic resonance imaging in dogs

Parameter	T2W	FLAIR	GM selective 3D DIR	WM selective 3D DIR
TR (ms)	5904	8000	5000	5000
TE (ms)	80	100	80	80
TI (ms)	-	2433	2562/605	2290/419
ETL	20	20	140	140
ST (mm)	3	3	2	2
Locs per slab	-	-	50	50
FOV (mm)	200	200	200	200
Matrix	288 × 224	256 × 192	176 × 176	176 × 176
NEX	4	2	2	2
Acquisition time (min:sec)	4:49	8:1	5:24	5:23

TR, repetition time; TE, echo time; TI, inversion time; ETL, echo train length; ST, slice thickness; FOV, field-of-view; NEX, number of excitations; T2W, T2-weighted; FLAIR, fluid attenuated inversion recovery; DIR, double inversion recovery; 3D, three-dimensional; GM, gray matter; WM, white matter

3. Data analysis

The qualitative and quantitative analysis of brain images were conducted using a DICOM viewer software (RadiAnt DICOM Viewer, version 4.6.9, free evaluation edition, Medixant, Poznan, Poland). The qualitative analysis was performed by one veterinarian (M.S.J.) with 2 years of radiology experience, under the supervision of a veterinarian (J.H.Y.) with diagnostic imaging expertise. The quantitative measurements were performed by three other veterinarians (M.S.J, S.H.Y., and D.J.L.) with 1-2 years of radiology experience. Because of obvious signal differences, the readers could not be entirely blinded to the type of the sequences.

In qualitative assessment, all MR images were evaluated at the six different transverse planes; at the level of the frontal lobe, optic chiasm, interthalamic adhesion, mesencephalic aqueduct, pons, and medulla oblongata. For each plane, distinction between gray and white matter was assessed using a four-point scale (Table 2). In addition, the readers assessed presence and severity of the artifacts, including motion, partial volume averaging, and flow artifacts. Transverse images of gray and white matter selective 3D DIR sequence were reconstructed using multiplanar reconstruction, then sagittal and dorsal planes were assessed for the presence of section to section signal intensity variations along the slab direction.

In quantitative assessment, contrast ratios (CRs), signal-to-noise ratios (SNRs), and contrast-to-noise ratios (CNRs) of the GM, WM and CSF were calculated as follows:

$$CR_{tissue\ 1,\ 2} = (SI_{tissue\ 1} - SI_{tissue\ 2}) / (SI_{tissue\ 1} + SI_{tissue\ 2})$$

$$SNR_{tissue} = SI_{tissue} / SD_{air}$$

$$CNR_{tissue\ 1,\ 2} = (SI_{tissue\ 1} - SI_{tissue\ 2}) / SD_{air}$$

where SI_{tissue} is the mean tissue signal intensity; SD_{air} the standard deviation of background signal. The CRs and CNRs are calculated using the absolute value because a positive or a negative contrast between the two tissues is considered to be equal (Usamentiaga et al., 2018). All values are given as mean ± SD. Signal intensities of individual types of tissues were assessed by region of interest (ROI) measurements with the ROI placed identically on each sequence (Fig. 1). The gray and white matter ROIs were chosen from the thickest and most uniform area possible, the CSF measurement was taken within the lateral ventricles. Standard deviation (SD) of background was determined by measuring the SD of the pixel intensities in a background air containing no image artifacts.

Table 2. Qualitative assessment criteria for gray-white matter distinction

Factor	Criteria
Distinction between gray and white matter	1= not visualized at all 2= poorly visualized but possible to detect 3= clearly visualized with blurry junction 4= clearly visualized with sharp junction

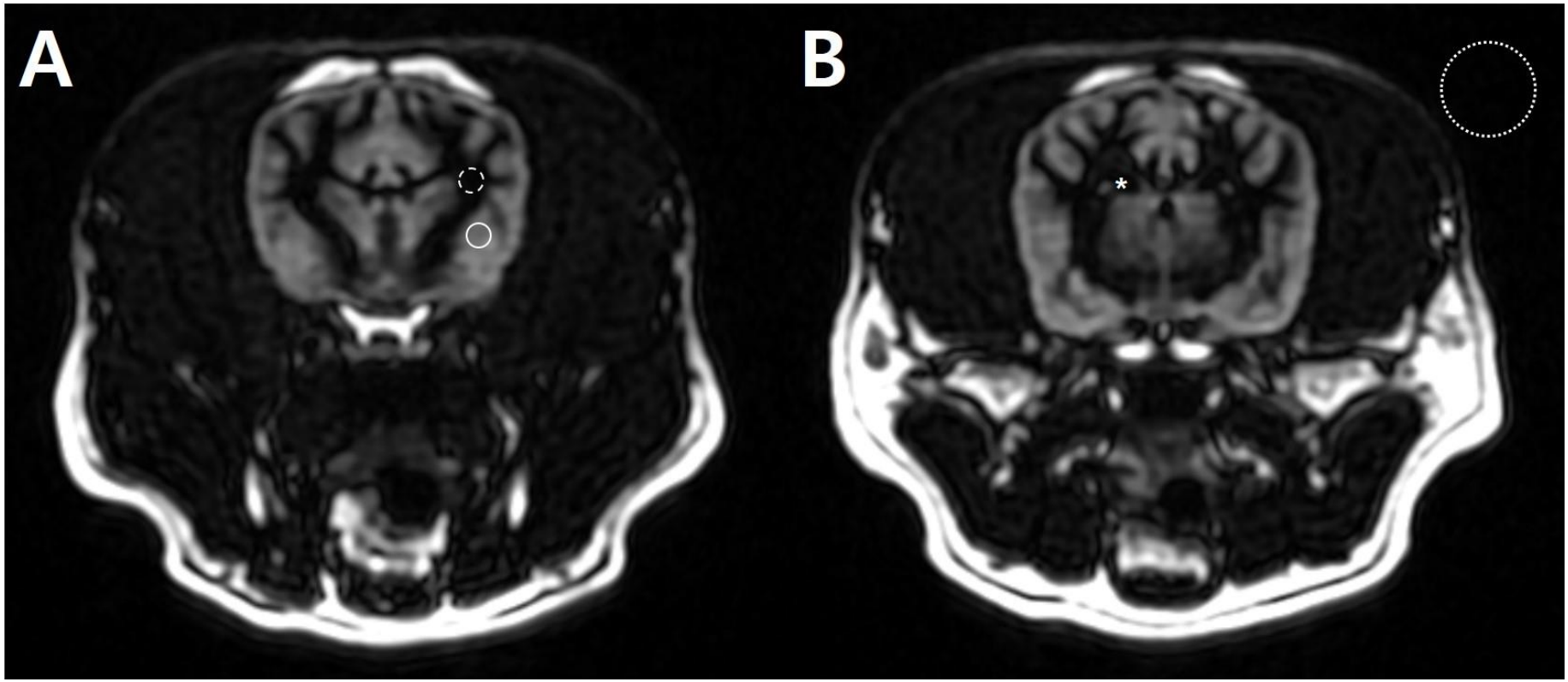

Figure 1. Transverse gray matter selective three-dimensional double inversion recovery images at the level of the optic chiasm (A) and interthalamic adhesion (B) in a dog. The regions of interest (ROI) of gray and white matter were chosen from the thickest and most uniform area possible (solid line and dashed line). The ROI for CSF measurement was taken within the lateral ventricles (asterisk). Standard deviation of background was measured in a background air containing no image artifacts (dotted line).

4. Statistical analysis

All statistical analysis was conducted by one author with diagnostic imaging expertise and statistical training (M.S.J.) using commercially available software (SPSS statistical program, IBM SPSS Statistics 25, IBM Corporation, NY). All the parameters were compared using the Kruskal-Wallis H test and post hoc test with Bonferroni correction. Interobserver agreements between the three observers were assessed using the interclass correlation coefficient (ICC) test. Variables with *P*-values of < 0.05 were considered statistically significant.

Results

Brain MR images were successfully attained with each sequence in all dogs without any anesthetic complications. The total scan time was approximately 25-30 min in each dog. The acquisition time of each sequence is presented in Table 1.

The score of gray-white matter distinction is displayed for each pulse sequence and each location (Table 3). In all six locations from the frontal lobe to the medulla oblongata level, gray-white matter distinction was more clearly visualized on GM selective 3D DIR than T2W and FLAIR. GM selective 3D DIR also had statistically higher distinction score than WM selective 3D DIR at the level of the mesencephalic aqueduct and pons. WM selective 3D DIR did not have significant difference with T2W and FLAIR from the frontal lobe to the pons level, but showed significantly higher distinction score than T2W and FLAIR at the level of the medulla oblongata. T2W and FLAIR tended to blur gray-white matter distinction of the occipital lobe at the medulla oblongata level, and the border of gray and white matter was even not visible at all in some FLAIR images. On the other hand, 3D DIR sequences, both GM and WM selective, clearly visualized gray-white matter distinction at that region (Fig. 2). FLAIR generally showed poor gray-white matter distinction except for the interthalamic adhesion level, and the distinction score was particularly low at the medulla oblongata level.

Motion and flow artifacts were absent, regardless of the sequence in all dogs. On the other hand, partial volume averaging artifacts were detected at the all sequences. The severity of partial volume averaging artifacts was mild at 3D DIR

images, compared to T2W and FLAIR. These artifacts were usually identified at the narrow sulci and gyri region. FLAIR images were more severely affected by partial volume averaging artifacts than other sequences, and these artifacts resulted in blurring of the gray-white matter junctions (Fig. 3).

By the single-slab excitation, 3D DIR images had homogeneous signal intensity along the slab direction without section to section variations. Thus, the reconstructed sagittal and dorsal images of GM and WM selective 3D DIR sequences had same spatial resolution as the original transverse images, without any image degradation (Fig. 4).

For the measurements of quantitative parameters including CRs, SNRs, and CNRs, the interclass correlation among the three readers showed excellent interobserver agreement (Table 4). The mean and SD for CR, SNR, and CNR of the GM, WM and CSF are displayed for each pulse sequence (Table 5). $CR_{GM\text{-}WM}$ was markedly higher for GM and WM selective 3D DIR than T2W and FLAIR, and FLAIR had the lowest $CR_{GM\text{-}WM}$ than other three sequences. $CNR_{GM\text{-}WM}$ of GM and WM selective 3D DIR sequences were significantly higher than FLAIR. Although the mean values of $CNR_{GM\text{-}WM}$ of both 3D DIRs were measured to be higher than T2W, differences were not statistically significant. There were no significant differences in $CR_{GM\text{-}WM}$ and $CNR_{GM\text{-}WM}$ between GM and WM selective 3D DIR. $CR_{GM\text{-}CSF}$ of GM selective DIR was significantly higher than T2W, but there was no significant difference with FLAIR. $CR_{WM\text{-}CSF}$ was significantly higher in WM selective DIR than both T2W and FLAIR. $CNR_{GM\text{-}CSF}$ of GM selective DIR and $CNR_{WM\text{-}CSF}$ of WM selective DIR have no statistical differences with T2W and FLAIR. No significant difference was found between sequences for SNR_{GM} except

WM selective DIR, which suppressed GM signals. Likewise, no significant difference was found between sequences for SNR_{WM} except GM selective DIR, which suppressed WM signals.

Table 3. Comparison of MR sequences for gray-white matter distinction score at six different locations

	T2W (median (range))	FLAIR (median (range))	GM selective 3D DIR (median (range))	WM selective 3D DIR (median (range))	*P*-value
Frontal lobe	3 (0)[a]	2 (1.0)[b]	4 (0)[a, b]	3 (1.0)	0.002
Optic chiasm	3 (0)[a]	2 (1.0)[b]	4 (0)[a, b]	3 (1.0)	0.002
Interthalamic-adhesion	3 (0)[a]	3 (1.0)[b]	4 (0)[a, b]	3 (1.0)	0.002
Mesencephalic-aqueduct	3 (0)[a]	2 (1.0)[b]	4 (0)[a, b, c]	3 (1.0)[c]	0.001
Pons	3 (1.0)[a]	2 (0)[b]	4 (0)[a, b, c]	3 (1.0)[c]	0.002
Medulla-oblongata	2 (0)[a, b]	1 (1.0)[c, d]	4 (1.0)[a, c]	3 (0)[b, d]	0.001

T2W, T2-weighted; FLAIR, fluid attenuated inversion recovery; DIR, double inversion recovery; 3D, three-dimensional; GM, gray matter; WM, white matter

[a, b, c] Within a row, the same superscript indicated statistically significant differences between two groups using a Bonferroni correction (significance level of *P*-value < 0.0083)

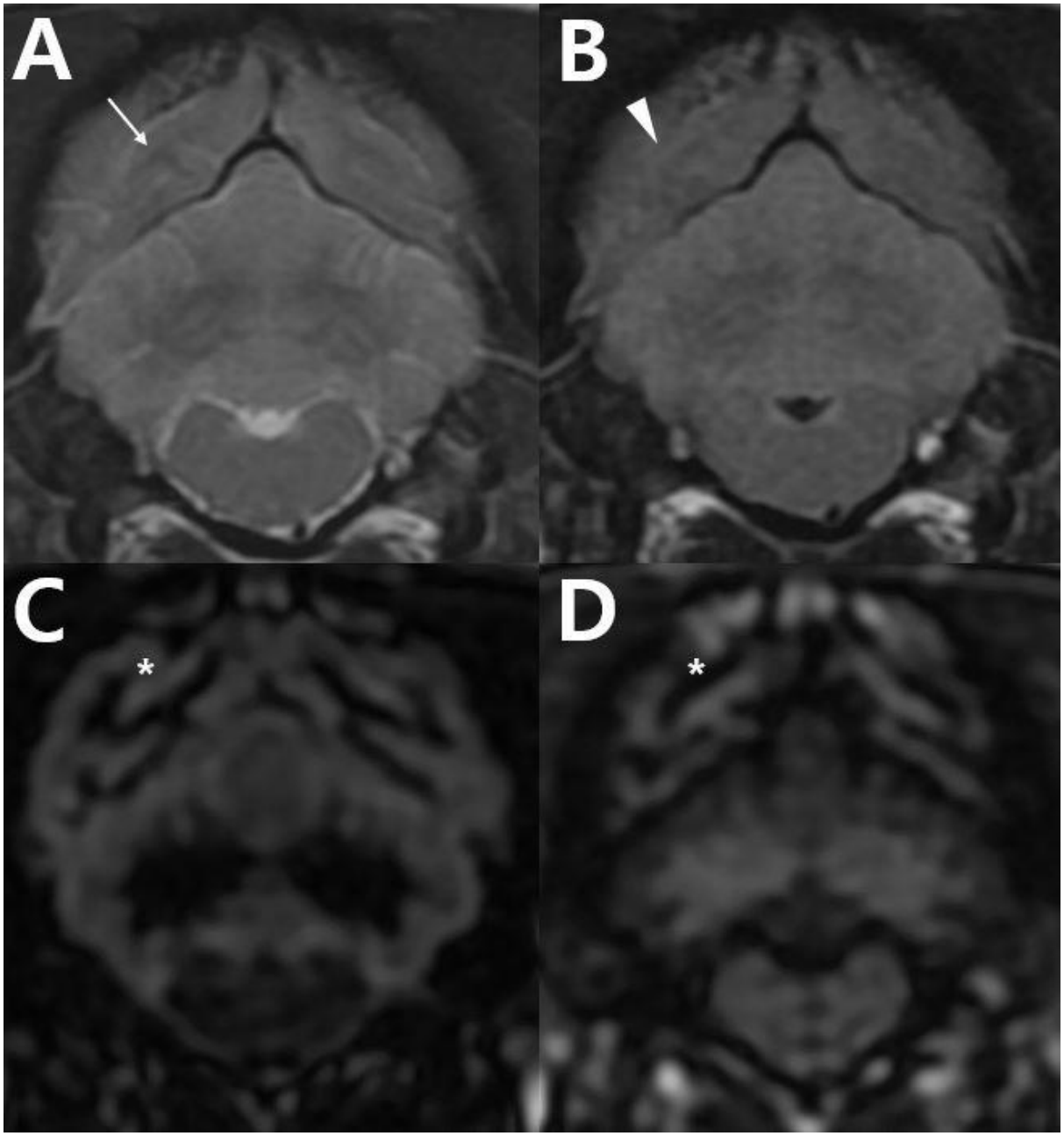

Figure 2. Transverse T2-weighted (T2W, A), fluid attenuated inversion recovery (FLAIR, B), gray matter selective three-dimensional double inversion recovery (GM selective 3D DIR, C), and white matter selective three-dimensional double inversion recovery (WM selective 3D DIR, D) images at the level of the medulla oblongata in a dog. T2W and FLAIR images showed blurry gray-white matter distinction (arrow and arrowhead), while GM and WM selective 3D DIR images clearly visualized the border of gray and white matter (asterisk) at the level of the medulla oblongata.

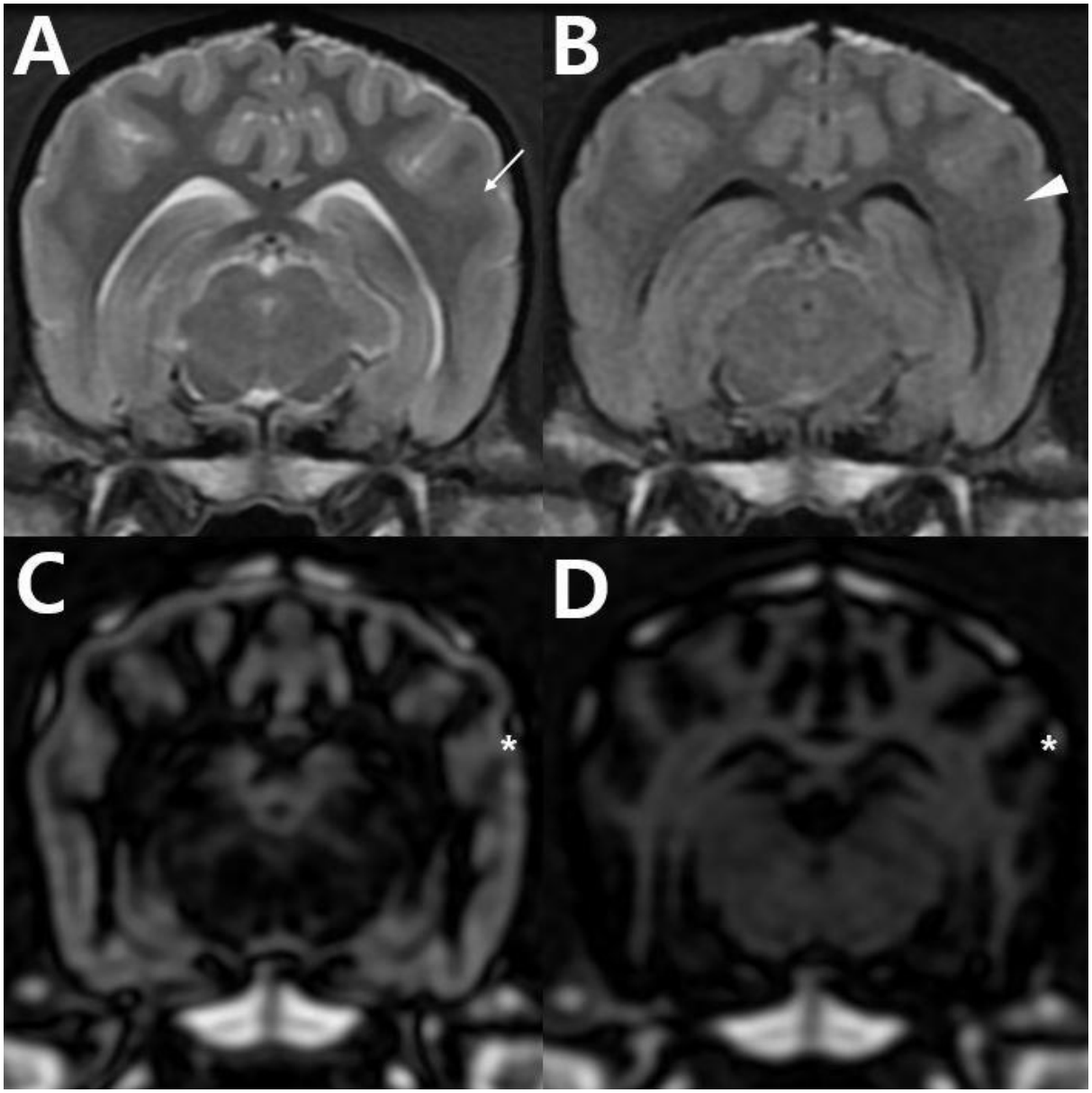

Figure 3. Transverse T2-weighted (T2W, A), fluid attenuated inversion recovery (FLAIR, B), gray matter selective three-dimensional double inversion recovery (GM selective 3D DIR, C), and white matter selective three-dimensional double inversion recovery (WM selective 3D DIR, D) images at the identical level in a dog. Partial volume averaging artifacts at the gray-white matter junctions were more severe in T2W (arrow) and FLAIR (arrowhead) than GM and WM selective 3D DIR (asterisk) images, resulting in blurred gray-white matter distinction.

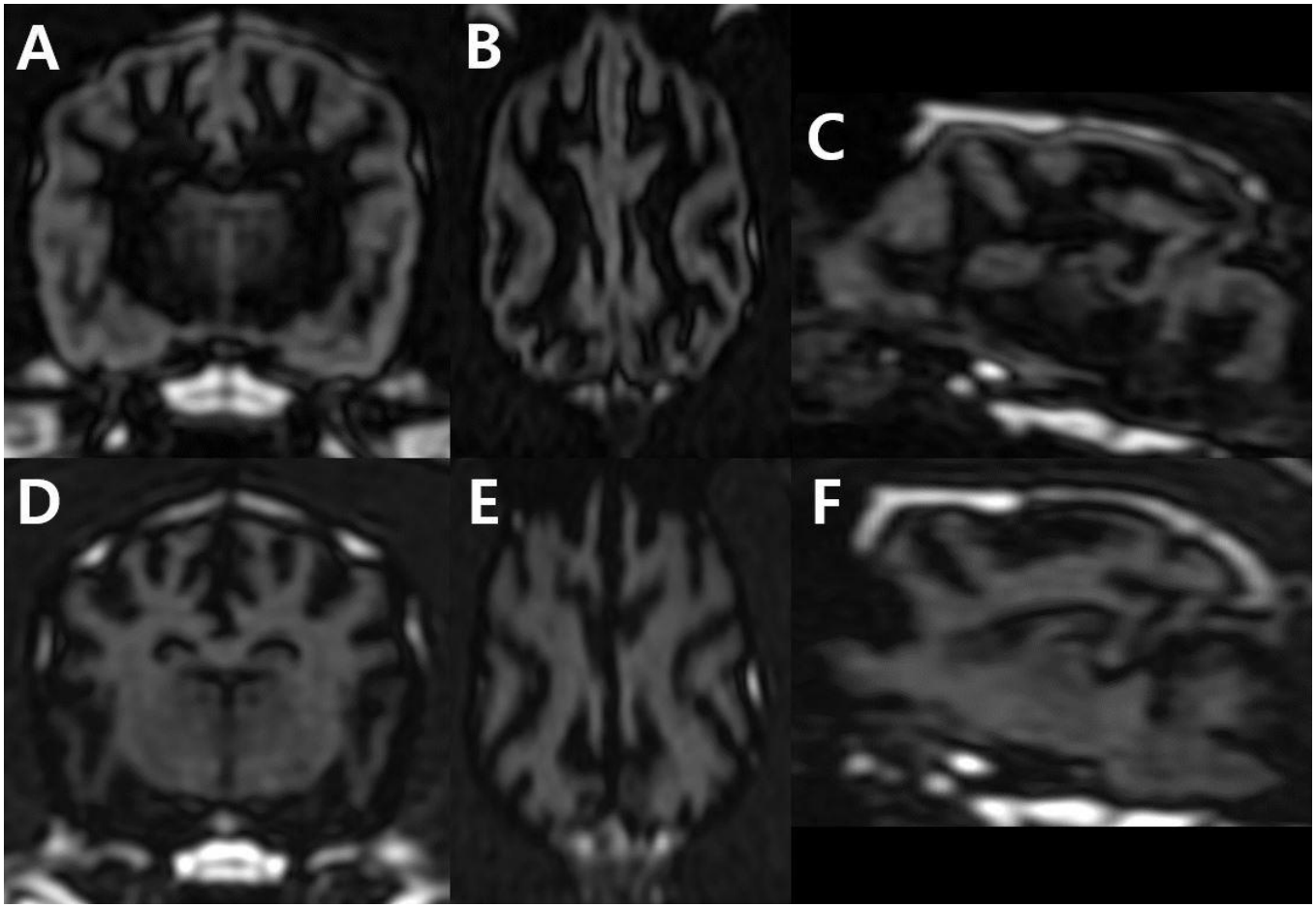

Figure 4. Gray matter selective three-dimensional double inversion recovery (GM selective 3D DIR, A-C) and white matter selective three-dimensional double inversion recovery (WM selective 3D DIR, D-F) images in a dog. Because of the nearly isotrophic resolution, reconstructed images of GM selective 3D DIR (B, C) and WM selective 3D DIR (E, F) had identical image quality with the original transverse magnetic resonance images (A, D).

Table 4. Interclass correlation coefficient values for interobserver reliability of quantitative analysis

Evaluation factors		ICC	95% confidence interval
	GM-WM	0.998	0.996-0.999
CR	GM-CSF	0.987	0.972-0.994
	WM-CSF	0.992	0.984-0.997
	GM	0.940	0.875-0.975
SNR	WM	0.952	0.899-0.979
	CSF	0.979	0.955-0.991
	GM-WM	0.987	0.973-0.995
CNR	GM-CSF	0.986	0.970-0.994
	WM-CSF	0.984	0.967-0.993

Table 5. Comparison of MR sequences for contrast between brain tissues

	Ratio	T2W (mean ± SD)	FLAIR (mean ± SD)	GM selective DIR (mean ± SD)	WM selective DIR (mean ± SD)	*P*-value
GM	SNR	183.28 ± 43.383[a]	122.22 ± 32.306[b]	137.04 ± 54.595[c]	17.95 ± 4.712[a, b,c]	0.004
WM	SNR	114.27 ± 26.308[a]	83.77 ± 24.002[b]	15.01 ± 6.413[a, b, c]	146.43 ± 46.560[c]	0.004
CSF	SNR	315.05 ± 81.312[a, b, c]	21.30 ± 5.609[a]	16.00 ± 7.239[b]	19.90 ± 4.693[c]	0.007
GM-WM	CR	0.23 ± 0.018[a, b]	0.19 ± 0.020[a, b]	0.80 ± 0.042[a]	0.77 ± 0.044[b]	0.001
	CNR	69.02 ± 17.952[a]	38.45 ± 9.305[a, b, c]	122.03 ± 49.147[b]	128.48 ± 43.405[c]	0.002
GM-CSF	CR	0.26 ±0.028[a, b]	0.70 ± 0.047[a]	0.79 ± 0.030[b]	0.10 ± 0.052[a, b]	0.001
	CNR	131.77 ± 40.783[a]	100.91 ± 27.695[b]	121.03 ± 47.701[c]	3.87 ± 2.199[a, b, c]	0.009
WM-CSF	CR	0.47 ± 0.011[a]	0.59 ± 0.064[a]	0.12 ± 0.076[a]	0.75 ± 0.043[a]	0.000
	CNR	200.78 ± 55.178[a]	62.46 ± 19.417[a]	3.45 ± 1.897[a, b]	126.53 ± 42.889[b]	0.001

SNR, signal to noise ratio; CR, contrast ratio; CNR, contrast to noise ratio; T2W, T2-weighted; FLAIR, fluid attenuated inversion recovery; DIR, double inversion recovery; 3D, three-dimensional; GM, gray matter; WM, white matter

[a, b, c] Within a row, the same superscript indicated statistically significant differences between two groups using a Bonferroni correction (significance level of *P*-value < 0.0083)

Discussion

Based on the author's literature review, this is the first published study of the utility of 3D DIR sequences for brain imaging in clinically healthy dogs. In this study, we compared the brain images obtained by single-slab 3D DIR sequences with those of conventional sequences, T2W and FLAIR, qualitatively and quantitatively.

Our findings showed that GM selective 3D DIR is superior to conventional T2W and FLAIR in delineating the boundaries between gray and white matter in the overall brain area. This finding is in an agreement with human studies that reported GM selective DIR provides a better gray-white differentiation than T2W or FLAIR (Redpath et al., 1994; Turetschek et al., 1998). Whereas WM selective 3D DIR had no significant difference from the conventional sequences in visualization of gray-white matter distinction, from the frontal lobe to the pons level. However, at the level of the medulla oblongata, where T2W and FLAIR images showed severe blurring of the brain tissue, not only GM selective 3D DIR but also WM selective 3D DIR provided much better visualization of the boundaries between gray and white matter. This is because 3D DIR sequences are much less affected by partial volume averaging artifacts than other sequences at the medulla oblongata level.

In our study, artifacts such as motion or flow artifacts were not visually apparent on 3D DIR images, except for mild partial volume averaging artifacts. According to the previous study, it is reported that nonselective excitation of the single-slab 3D DIR can prevent the occurrence of artifacts from blood flow or CSF

pulsation (Pouwels et al., 2006).

A further advantage of this sequence is that isotrophic resolution of 3D sequence allows the original images to be reconstructed in any orientation with same spatial resolution. Thus, 3D DIR sequences could eliminate the need to repeat MR examinations with identical region in different planes.

In quantitative analysis, GM selective 3D DIR had significantly higher $CR_{GM\text{-}WM}$ than other conventional sequences, T2W and FLAIR. In addition, GM selective 3D DIR had higher mean value of $CR_{GM\text{-}CSF}$ than T2W and FLAIR, but showed no statistical difference with FLAIR, a sequence that suppresses the CSF signal. WM selective 3D DIR showed significantly higher $CR_{GM\text{-}WM}$ and $CR_{WM\text{-}CSF}$ than other conventional sequences. These results revealed that good degrees of unwanted signal suppression were achieved with both two 3D DIR sequences. A previous study reported that CSF suppression of WM selective DIR was poorer than GM selective DIR in the normal human brain (Redpath et al., 1994). But in our study, no significant difference of CSF suppression was found between two 3D DIR sequences.

CNR, a parameter which takes into account the background noise, is regarded as clinically the most relevant parameter, and the ability to detect brain anatomy depends on CNR (Duyn et al., 2007; Runge, 2009). In our study, both GM and WM selective 3D DIR had significantly higher $CNR_{GM\text{-}WM}$ than FLAIR. It suggests that both two 3D DIR sequences provide better contrast resolution between gray and white matter than FLAIR. In addition, the mean values of $CNR_{GM\text{-}WM}$ of two 3D DIR sequences were higher than that of T2W, but differences were statistically non-significant. $CNR_{GM\text{-}CSF}$ of GM selective 3D DIR and $CNR_{WM\text{-}}$

$_{CSF}$ of WM selective 3D DIR had no significant differences with other sequences, and even T2W had higher mean values of CNR_{GM-CSF} and CNR_{WM-CSF} than 3D DIR sequences. Therefore, 3D DIR sequences may not be superior for delineating the boundary between CSF regions such as ventricles or subarachnoid space and brain parenchyma. FLAIR showed significantly the lowest CR_{GM-WM} and CNR_{GM-WM}, which suggests that the ability of gray-white matter differentiation would be the worst.

The previous studies stated long scan time may limit the routine clinical use of the DIR sequences (Redpath et al., 1994; Turetschek et al., 1998). In the current study, the parameters of 3D DIR sequences were adjusted for the acquisition time to be clinically acceptable. One of those, number of excitations (NEX) was adjusted from 4 to 2 because subjectively there was no significant difference in quality between images with NEX of 4 and NEX of 2. As a result, the scan time was cut in half and both GM and WM selective 3D DIR acquired shorter scan time (5 minutes 24 seconds in GM selective 3D DIR and 5 minutes 23 seconds in WM selective 3D DIR) than FLAIR (8 minutes 1 seconds). We assumed that adjustment of the parameters for reducing the scan time might cause substantial loss of SNR. But in our study, SNR_{GM} of GM selective 3D DIR and SNR_{WM} of WM selective 3D DIR had no statistical difference with other sequences. This result is different from the previous studies, which revealed that DIR sequences had relatively low SNRs (Turetschek et al., 1998; Pouwels et al., 2006).

Our study had some limitations. Sample size was small and only clinically healthy dogs were enrolled. Several CNS diseases in human are known to cause changes in GM, and numerous studies have reported that 3D DIR sequence is

useful for evaluating these diseases (Boulby et al., 2004). Likewise, in veterinary medicine, there are diseases that cause changes in GM, and the representative one is epilepsy (Frank et al., 2018). A study found the reduction of GM in dogs with idiopathic and structural epilepsy, by using voxel based morphometry (VBM) analysis (Frank et al., 2018). For VBM to function properly, the MRI image should have good contrast between the different brain tissues. However, the tissue distinction is not accurate especially in the central GM region, which have signal intensities that are similar to WM. Another problem is that the voxels containing several tissues may not be interpreted accurately, because the VBM model assumes that all voxels contain only one type of tissue (Ashburner et al., 2000). Considering the characteristics of 3D DIR sequences that can provide high contrast between gray and white matter with less partial volume averaging, using 3D DIR images for VBM could potentially resolve these problems. In addition, 3D DIR sequences are expected to provide superior conspicuity of brain lesions located at the gray-white matter junction, and the diagnostic efficacy of 3D DIR sequences for brain lesions such as meningoencephalitis should be studied further.

Conclusion

Single-slab 3D DIR sequences, both GM and WM selective, provided higher contrast between gray and white matter with less imaging artifacts than conventional sequences including T2W and FLAIR. Thus, the addition of a single-slab 3D DIR sequences to a standard MR brain imaging protocol may be useful for enhanced anatomic contrast depiction. This study can also provide the background data for further studies about DIR sequences for evaluating brain diseases in dogs, therefore further studies are warranted using dogs with brain lesions.

References

Almutairi, A. D., Hassan, H. A., Suppiah, S. Alomair, OI., Alshoaibi, A., Almutairi, H., Mahmud R., 2020. Lesion load assessment among multiple sclerosis patient using DIR, FLAIR, and T2WI sequences. Egyptian Journal of Radiology and Nuclear Medicine 51, 209.

Ashburner, J., Friston, K. J., 2000. Voxel-based morphometry - The methods. NeuroImage 11, 805–821.

Bedell, B. J., Narayana, P. A., 1988. Implementation and evaluation of a new pulse sequence for rapid acquisition of double inversion recovery images for simultaneous suppression of white matter and CSF. Journal of Magnetic Resonance Imaging 8, 544-547.

Boulby, P. A., Symms, M. R., Barker, G. J., 2004. Optimized interleaved whole-brain 3D double inversion recovery (DIR) sequence for imaging the neocortex. Magnetic Resonance in Medicine 51, 1181–1186.

Duyn, J. H., Van Gelderen, P., Li, T. Q., De Zwart, J. A., Koretsky, A. P.,

Fukunaga, M., 2007. High-field MRI of brain cortical substructure based on signal phase. Proceedings of the National Academy of Sciences of the United States of America 104, 11796-11801.

Frank L, Lüpke M, Kostic D, Löscher W, Tipold A., 2018. Grey matter volume in healthy and epileptic beagles using voxel-based morphometry - a pilot study. BMC Veterinary Research 14, 50.

Geurts, J. J. G., Pouwels, P. J. W., Uitdehaag, B. M. J., Polman, C. H., Barkhof, F., Castelijns, J. A., 2005. Intracortical lesions in multiple sclerosis: Improved detection with 3D double inversion-recovery MR imaging. Radiology 236, 254–260.

Hamed, W., Fathi, W., Mahmoud, W., Elhawary, G., 2019. Diagnostic accuracy of double inversion recovery in delineation of multiple sclerosis lesions and its clinical correlation with expanded disability scoring system. Egyptian Journal of Radiology and Nuclear Medicine 50, 114.

Hecht, S., Adams, W. H., 2010. MRI of brain disease in veterinary patients part 1: Basic principles and congenital brain disorders. Veterinary Clinics of North America: Small Animal Practice 40, 21–38.

Jahng, G. H., Lee, D. K., Lee, J. M., Rhee, H. Y., Ryu, C. W., 2016. Double inversion recovery imaging improves the evaluation of gray matter volume losses in patients with Alzheimer's disease and mild cognitive impairment. Brain Imaging and Behavior 10, 1015–1028.

Kraft, S. L., Gavin, P. R., Wendling, L. R., Reddy, V. K., 1989. Canine brain anatomy on magnetic resonance images. Veterinary Radiology 30, 147-158.

Mai, W. 2018. Diagnostic MRI in Dogs and Cats, First Edn. CRC Press, NW, USA, pp. 75-700.

Pouwels, P. J. W., Kuijer, J. P. A., Mugler, J. P., Guttmann, C. R. G., Barkhof, F., 2006. Human gray matter: Feasibility of single-slab 3D double inversion-recovery high-spatial-resolution MR imaging. Radiology 241, 873–879.

Redpath, T. W., Smith, F. W., 1994. Technical note: Use of a double inversion recovery pulse sequence to image selectively grey or white brain matter. The British Journal of Radiology 67, 1258-1263.

Robertson I., 2011. Optimal magnetic resonance imaging of the brain. Veterinary

Radiology and Ultrasound 52, 15-22.

Runge, V. M., Nitz, W. R., Schmeets, S. H., 2009. The Physics of Clinical MR Taught Through Images, Second Edn. Thieme, NW, USA, pp. 26-29.

Sun, K., Yu, T., Yang, D., Ren, Z., Qiao, L., Ni, D., Wang, X., Zhao, Y., Chen, X., Xiang, J. et al., 2021. Fluid and white matter suppression imaging and voxel-based morphometric analysis in conventional magnetic resonance imaging - Negative epilepsy. Frontiers in Neurology 12, 651592.

Turetschek, K., Wunderbaldinger, P., Bankier, A. A., Zontsich, T., Graf, O., Mallek, R., Hittmair, K., 1998. Double inversion recovery imaging of the brain: initial experience and comparison with fluid attenuated inversion recovery imaging. Magnetic Resonance Imaging 16, 127-135.

Umino, M., Maeda, M., Ii, Y., Tomimoto, H., Sakuma, H., 2019. 3D double inversion recovery MR imaging: Clinical applications and usefulness in a wide spectrum of central nervous system diseases. Journal of Neuroradiology 46, 107–116.

Usamentiaga, R., Ibarra-Castanedo, C., Maldague, X., 2018. More than fifty shades

of grey: quantitative characterization of defects and interpretation using SNR and CNR. Journal of Nondestructive Evaluation 37, 25.

국문초록

임상적으로 건강한 개에서 단일 슬랩 삼차원 이중역전회복을 이용한 뇌 자기공명영상 평가

서울대학교 대학원
수의학과 임상수의학 전공
제 미 성

수의학에서 자기공명영상은 뇌 영상화에 널리 이용된다. 그러나 뇌 조직의 복잡한 구조로 인해 기존의 시퀀스에서는 부분 용적 평균화와 같은 허상의 문제가 발생하였다. 이에 대한 해결 방안으로서 인의에서는 이중역전회복 시퀀스에 대한 여러 연구가 보고되어 있다. 그러나 개에서 이중역전회복 시퀀스를 이용한 뇌 자기공명영상에 대한 임상 연구는 아직까지 이루어지지 않았다. 본 연구의 목적은 임상적으로 건강한 개에서 단일 슬랩 삼차원 이중역전회복을 이용한 뇌 자기공명영상의 특징을 평가하는 것이다.

다섯 마리의 비글견을 대상으로 각각 (1)스핀에코 T2강조, (2) 액체감쇠역전회복, (3)회색질 선택적 단일 슬랩 삼차원 이중역전회복,

(4)백색질 선택적 단일 슬랩 삼차원 이중역전회복 시퀀스를 이용한 자기공명영상 평가가 이루어졌다. 영상에 대한 정성 분석을 위해, 각각의 시퀀스에서 회색질과 백색질의 경계가 구별되는 정도, 허상의 유무 및 그 정도가 평가되었다. 이와 더불어 단일 슬랩 삼차원 이중역전회복을 이용하여 획득한 영상을 다중 단면 재구성하여 각 영상의 품질을 비교 평가하였다. 한편 정량 분석을 위해서는 각각의 시퀀스에서 대조도비, 신호 대 잡음비, 그리고 대조도 대 잡음비가 측정되었다.

회색질 선택적 단일 슬랩 삼차원 이중역전회복은 뇌의 전반적인 영역에 걸쳐 회색질과 백색질의 경계를 구별하는 데에 있어 스핀에코 T2강조 및 액체감쇠역전회복보다 더 우수하였다. 반면, 백색질 선택적 단일 슬랩 삼차원 이중역전회복은 연수 수준에서 다른 두 시퀀스보다 회색질과 백색질의 경계를 더 잘 구별하였는데, 스핀에코 T2강조 및 액체감쇠역전회복 영상의 경우 연수 수준에서 심한 부분 용적 평균화 허상을 보여 회색질과 백색질의 경계가 잘 구별되지 않았다. 회색질 그리고 백색질 선택적 삼차원 이중역전회복 영상은 다른 시퀀스들에 비해 허상의 발생이 적은 경향을 보였으며, 가로 단면 영상으로부터 다중 단면 재구성된 시상면 및 등단면 영상들은 품질의 저하 없이 원본 영상과 동일한 공간 해상도를 보였다. 회색질 및 백색질 선택적 단일 슬랩 삼차원 이중역전회복은 원하지 않는 신호를 억제함으로써 회색질과 백색질 사이에서 유의적으로 높은 대조도를 보였다. 본 연구로부터 확인된 결과들을 토대로, 추후 뇌 질환이 있는 개에서 이중역전회복을 이용한 자기공명영상

평가가 가능할 것으로 기대된다.

주요어: 뇌, 이중역전회복, 자기공명영상, 개

학 번: 2021-23751